Proceedings of the ASME 2014 Conference on Smart Materials, Adaptive Structures and Intelligent Systems
SMASIS2014
September 8-10, 2014, Newport, Rhode Island, USA

SMASIS2014-7431

DESIGN OF RECTIFIED PIEZOELECTRIC POWER GENERATORS BY FINITE ELEMENT METHODS

P. H. Wu and Y. C. Shu*
Institute of Applied Mechanics
National Taiwan University
Taipei 106, Taiwan, R.O.C.

ABSTRACT

The article proposes designing rectified piezoelectric power generators based on the direct finite element method. It accounts for the consideration of common interface circuits such as the standard and parallel-/series-SSHI (synchronized switch harvesting on inductor) circuits, and complicated structural configurations such as arrays of piezoelectric oscillators. The proposed model suggests replacing the energy harvesting circuit by an equivalent load impedance in series with negative piezoelectric capacitance. As the expression of the equivalent load impedance can be explicitly derived, the proposed finite element approach is capable of handling common interface circuits without resorting to circuit solvers. Finally, the model is extended to the consideration of SECE (synchronized electric charge extraction) circuit which offers an advantage of independence of harvested power on external loads.

INTRODUCTION

Tremendous efforts have been made for developing vibration-based piezoelectric energy harvesting due to the ubiquitous presence of ambient vibrations as well as high electromechanical coupling in piezoelectric materials [1, 2]. These include the design of optimal mechanical structures for transmitting environmental vibration to mechanical energy [3–14], the suitable choices of piezoelectric materials for converting strain energy to electric energy [15–19] and the optimal energy harvesting circuits for maximum power transfer [20–32]. However, the bottleneck for developing such techniques is that it requires the matching between the resonance of the system and the frequency of ambient vibration source. This gives rise to the need of designing structures with complex configurations for frequency tuning [33–40]. Another approach for enlarging bandwidth is to use multiple piezoelectric oscillators with slightly different resonances [41–43]. However, most works in this direction often neglect the importance of rectified interface circuits [44–47]. As a result, these research efforts raise an issue for needing a convenient numerical tool used for considering complicated configurations either in structures or circuits.

Commercial finite element solvers are capable of simulating the electromechanical response of a piezoelectric oscillator as long as the attached circuit element is linear. This gives rise to the estimation of AC power output that an energy harvester can achieve [48, 49]. However, the need of DC power output limits the application of finite element method to rectified piezoelectric elements. Hence, certain research efforts are made on the combination of finite element solvers and circuit simulators [50, 51]. These include the iteration method requiring constant data transfer between the finite element solver and circuit simulator, or the two-step approach requiring the finite element calculation of the system parameters used in the circuit simulation.

To avoid these inconveniences, a direct finite element model is proposed based on the use of equivalent load impedance. It suffices for the system-level design and takes into account practical energy harvesting circuits, such as the standard and parallel-/series-SSHI (synchronized switch harvesting on inductor) circuits. But different from the finite element method based the equivalent current model [52], the present approach is built on the equivalent voltage model. As a result, it can be extended

*Author for correspondence. Email: yichung@spring.iam.ntu.edu.tw.

Copyright © 2014 by ASME

Downloaded From: http://proceedings.asmedigitalcollection.asme.org/ on 08/12/2017 Terms of Use: http://www.asme.org/about-asme/terms-of-use

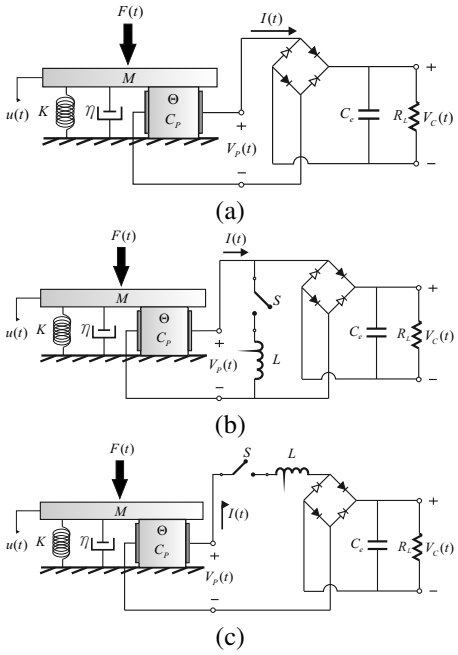

Figure 1. The parameter model of a piezoelectric power generator connected to (a) the standard interface, (b) the parallel-SSHI interface and (c) the series-SSHI interface.

to the case of multiple oscillators connected in series. In addition, the SECE (synchronized electric charge extraction) circuit commonly chosen in piezoelectric energy harvesting is also considered here.

Framework

Consider a piezoelectric device attached to some rectified energy harvesting circuit. Suppose it is excited at around resonance. The system is modeled as a mass + spring + damper + piezo-structure, with response governed by

$$M\ddot{u}(t)+\eta\dot{u}(t)+Ku(t)+\Theta V_p(t)=F(t), \quad (1)$$

$$-\Theta\dot{u}(t)+C_p\dot{V}_p(t)=-I(t), \quad (2)$$

where u is the displacement of mass M, V_p is the voltage across the piezoelectric device, $F(t)$ is the applied forcing function and $I(t)$ is the current flowing into the specified circuit, and η, K, Θ and C_p are the mechanical damping coefficient, the stiffness, the piezoelectric coefficient and the parasitic capacitance of the piezoelectric device, as illustrated in Fig. 1. To realize Eq. (2), consider an equivalent voltage V_p^* defined by

$$-\dot{V}_p^*+\dot{V}_p(t)=-\frac{1}{C_p}I(t) \text{ or } V_p^*-\frac{1}{C_p}\int Idt=V_p. \quad (3)$$

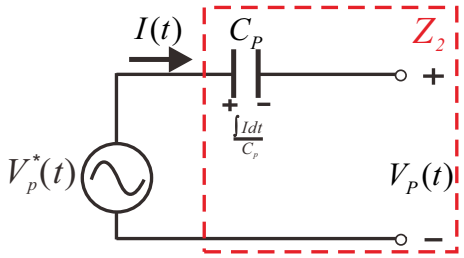

Figure 2. An equivalent voltage model where Z_2 is an equivalent load impedance of the circuit elements within the red rectangle.

where

$$V_p^*(t)=\frac{\Theta}{C_p}u(t), \quad \dot{V}_p^*(t)=\frac{\Theta}{C_p}\dot{u}(t). \quad (4)$$

The relation between the equivalent voltage V_p^* and the piezoelectric voltage V_p is illustrated in Fig. 2.

Next consider the standard harvesting circuit connected to the piezoelectric device. It consists of a rectifier followed by a filtering capacitance C_e for AC/DC conversion as shown in Fig. 1(a). The terminal load is a resistor R_L and V_c is the DC voltage across it. Notice that the perfect rectifying bridge is assumed here. Let $\bar{V}_p^*$ be the magnitude of $V_p^*(t)$ under the steady-state excitation with w as the applied frequency. Its relation with the DC output voltage V_c can be obtained from the consideration of the balance of charge as in Eq. (3). Indeed, it can be shown that [42]

$$V_c^{\text{Standard}}=\left(\frac{C_pwR_L}{\frac{\pi}{2}+C_pwR_L}\right)\bar{V}_p^* \quad (5)$$

for the case of standard interface. In addition, suppose the electronic interface circuit is replaced by other common circuits such as SSHI introduced by Guyomar and his coworkers [25]. Fig. 1(b) is the schematic of the parallel-SSHI which consists of adding up a switching device in parallel with the piezoelectric harvester device. Besides, Fig. 1(c) is the prototype of series-SSHI consisting of adding up a switching device in series with the piezoelectric element. Both cases are shown to be able to boost harvested power for weak electromechanical systems and can also be used for broadband improvement [22, 23]. The relation between $\bar{V}_p^*$ and V_c is shown in Eq. (6) and Eq. (7) [42]

$$V_c^{\text{P-SSHI}}=\left(\frac{C_pwR_L}{\frac{\pi}{2}+(\frac{1-q_I}{2})C_pwR_L}\right)\bar{V}_p^*, \quad (6)$$

$$V_c^{\text{S-SSHI}}=\left(\frac{C_pwR_L}{\frac{\pi}{2}(\frac{1-q_I}{1+q_I})+C_pwR_L}\right)\bar{V}_p^*, \quad (7)$$

Copyright © 2014 by ASME

Downloaded From: http://proceedings.asmedigitalcollection.asme.org/ on 08/12/2017 Terms of Use: http://www.asme.org/about-asme/terms-of-use

where $q_I = e^{-\frac{\pi}{2Q_I}}$ and Q_I is the electric quality factor for the measurement of energy loss from the inductor in series with the switch. Finally, the harvested average power $P_{\text{harvested}}$ is formulated by

$$P_{\text{harvested}} = \frac{V_c^2}{R_L}. \tag{8}$$

Now let Z_2 be the equivalent load impedance representing the piezoelectric capacitance and the rest of circuit elements, as demonstrated in the red rectangle in Fig. 2. This gives the relation between the equivalent voltage V_p^* and the current I by

$$V_p^* = I \cdot Z_2. \tag{9}$$

Further, from Eq. (3), Eq. (4) and Eq. (9), we have

$$\begin{aligned} V_p &= V_p^* - \frac{1}{C_p}\int I dt = V_p^* - \frac{1}{C_p Z_2}\int V_p^* dt \\ &= \frac{\Theta}{C_p}u - \frac{\Theta}{C_p^2 Z_2}\int u dt. \end{aligned} \tag{10}$$

Now, under the steady-state excitation, we may set

$$u(t) = \bar{u}e^{jwt}, \quad F(t) = \bar{F}e^{jwt}, \quad j^2 = -1, \tag{11}$$

where $\bar{u}$ and $\bar{F}$ are the complex magnitudes of displacement and forcing function. Therefore, substituting Eq. (10) into Eq. (1) with the help of Eq. (11) gives

$$\begin{aligned} \bar{u} &= \frac{\bar{F}}{K - w^2 M + \frac{\Theta^2}{C_p} + jw\eta + j\frac{\Theta^2}{C_p^2 w}(\frac{1}{Z_2})} \\ &= \frac{\bar{F}}{(K - w^2 M + \frac{\Theta^2}{C_p} + \frac{\Theta^2}{C_p^2 w}Y_{2\text{I}}) + j(w\eta + \frac{\Theta^2}{C_p^2 w}Y_{2\text{R}})}, \end{aligned} \tag{12}$$

where $Y_{2\text{R}}$ and $-Y_{2\text{I}}$ are the real and imaginary parts of the complex impedance $\frac{1}{Z_2}$; i.e.,

$$Y_2 = \frac{1}{Z_2} = Y_{2\text{R}} - jY_{2\text{I}}, \quad Y_{2\text{R}} = \text{Re}\{\frac{1}{Z_2}\}, \quad -Y_{2\text{I}} = \text{Im}\{\frac{1}{Z_2}\}. \tag{13}$$

Thus, the magnitude of displacement is

$$|\bar{u}| = \frac{\bar{F}}{\left\{\left(K - w^2 M + \frac{\Theta^2}{C_p} + \frac{\Theta^2}{C_p^2 w}Y_{2\text{I}}\right)^2 + \left(w\eta + \frac{\Theta^2}{C_p^2 w}Y_{2\text{R}}\right)^2\right\}^{\frac{1}{2}}}. \tag{14}$$

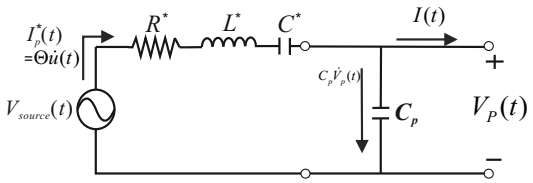

Figure 3. An equivalent circuit model stands for a piezoelectric oscillator.

However, the explicit expression of impedance Z_2 is still unknown. Fortunately, the same problem has been studied by Shu and Lien [20] who have shown that

$$|\bar{u}| = \frac{\bar{F}}{\left\{\left(K - w^2 M + \frac{w\Theta^2 R_L}{\frac{\pi}{2} + C_p w R_L}\right)^2 + \left(w\eta + \frac{2w\Theta^2 R_L}{\left(\frac{\pi}{2} + C_p w R_L\right)^2}\right)^2\right\}^{\frac{1}{2}}} \tag{15}$$

in the case of the standard interface. The comparison between Eq. (14) and Eq. (15) gives

$$Y_{2\text{R}}^{\text{Standard}} = \frac{2C_p^2 w^2 R_L}{\left(\frac{\pi}{2} + C_p w R_L\right)^2}, \quad Y_{2\text{I}}^{\text{Standard}} = -\frac{\frac{\pi}{2}C_p w}{\left(\frac{\pi}{2} + C_p w R_L\right)}. \tag{16}$$

Similarly, the same approach can be applied to the cases of SSHI circuits, giving rise to the formulations of the equivalent load impedance Z_2 for the parallel-SSHI

$$\begin{aligned} Y_{2\text{R}}^{\text{P-SSHI}} &= \frac{2C_p^2 w^2 R_L\left[1 + \frac{(1-q_I^2)}{2\pi}C_p w R_L\right]}{\left(\frac{\pi}{2} + \frac{(1-q_I)}{2}C_p w R_L\right)^2}, \\ Y_{2\text{I}}^{\text{P-SSHI}} &= -\frac{\frac{\pi}{2}C_p w}{\left(\frac{\pi}{2} + \frac{(1-q_I)}{2}C_p w R_L\right)}. \end{aligned} \tag{17}$$

and for the series-SSHI

$$Y_{2\text{R}}^{\text{S-SSHI}} = \frac{2C_p w}{\frac{\pi}{2}(\frac{1-q_I}{1+q_I}) + C_p w R_L}, \quad Y_{2\text{I}}^{\text{S-SSHI}} = 0. \tag{18}$$

FEM Model

An idea based on the use of the equivalent load impedance introduced in the previous section is proposed for finite element modeling of rectified piezoelectric energy harvesters. Indeed, Eq. (1) and Eq. (2) governing the response of a piezoelectric oscillator can be schematically presented by an equivalent circuit,

Copyright © 2014 by ASME

Downloaded From: http://proceedings.asmedigitalcollection.asme.org/ on 08/12/2017 Terms of Use: http://www.asme.org/about-asme/terms-of-use

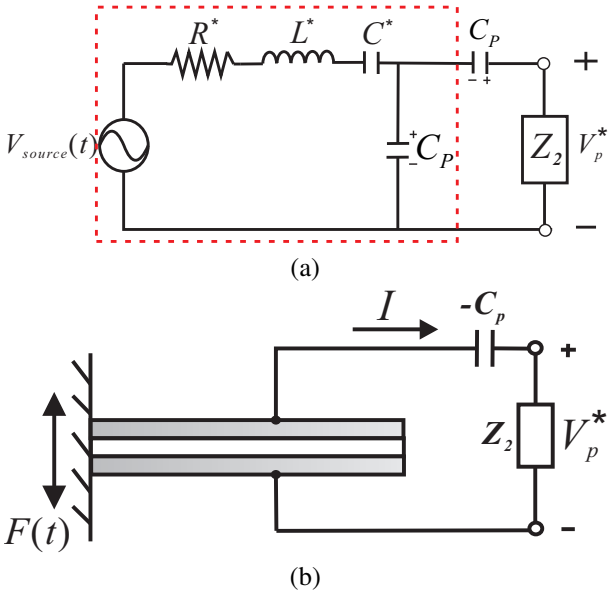

Figure 4. (a). An equivalent circuit model stands for the whole piezoelectric energy harvesting system. (b). Schematic presentation of a finite element model where the energy harvesting circuit is replaced by an equivalent load impedance in series with the negative piezoelectric capacitance.

as demonstrated in Fig. 3 where $R^* = \frac{\eta}{\Theta^2}$ is an equivalent resistance, $L^* = \frac{M}{\Theta^2}$ an inductance, $C^* = \frac{\Theta^2}{K}$ a capacitance, and $V_{\text{source}} = \frac{F}{\Theta}$ the voltage source [20]. Thus, combining Fig. 2 and Fig. 3 gives a full description of an equivalent circuit model standing for a piezoelectric energy harvesting system, as illustrated in Fig. 4(a) where Z_2 is the equivalent load impedance. Notice that the red rectangle in Fig. 4(a) models a piezoelectric oscillator. Hence, Fig. 4(a) can be explained as a harvester attached to a negative piezoelectric capacitance $(-C_p)$ in series with an equivalent load impedance Z_2. This gives the proposed finite element model schematically described by Fig. 4(b). In addition, the equivalent load impedance Z_2 is explicitly provided by Eq. (16), Eq. (17), and Eq. (18) for the standard, parallel-SSHI and series-SSHI interfaces. It is associated with the parameters including only the external load resistance R_L, excitation frequency w and the piezoelectric capacitance C_p. Thus, the model simulations can be carried out by any available commercial finite element softwares. As a result, the proposed approach provides a convenient tool for performance evaluation of a practical device. Finally, note that the voltage across the impedance Z_2 is not the real piezoelectric voltage V_p. It is the the equivalent voltage $V_p^*(t)$ defined by Eq. (4) whose magnitude is related to the DC output voltage V_c by Eq. (5), Eq. (6) and Eq. (7) for the standard, parallel-SSHI and series-SSHI interfaces, respectively. The harvested average power by Eq. (8) can therefore be

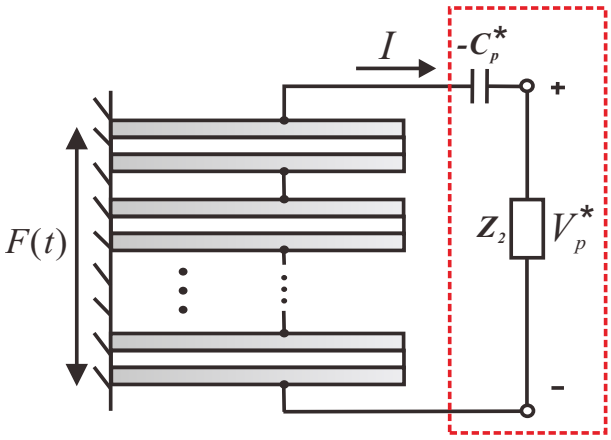

Figure 5. Schematic presentation of a finite element model for an array of piezoelectric oscillators connected in series. The energy harvesting circuit is replaced by an equivalent load impedance Z_2 in series with capacitance $-C_p^*$. Note that C_p^* is an overall capacitance of piezoelectric oscillators connected in series.

evaluated.

The proposed approach is not limited to the case of a single oscillator. Instead, it can be extended to the case of multiple piezoelectric oscillators. Indeed, suppose there are N number of piezoelectric oscillators connected in series. Let C_{p_i} denote the piezoelectric capacitance of the i oscillator. Therefore, the overall piezoelectric capacitance C_p^* is given by $\frac{1}{C_p^*} = \sum_{n=1}^{N} \frac{1}{C_{pn}}$. Further assume the array system is attached to a single rectified interface. Using the idea similar to that deriving the equivalent load impedance in the previous section, the impedance of the harvesting circuit in series with the overall piezoelectric capacitance is still Z_2 as in Eq. (16), Eq. (17), and Eq. (18) for various interfaces. Precisely, Fig. 5 describes a finite element model for a rectified array system. The inclusion of negative capacitance can be explained using the argument as the same as that in the case of a single oscillator. Finally, the DC output power of a rectified array system can be computed in the finite element environment as long as the excitation is harmonic with frequency at around to the resonance of the system.

Extension to SECE circuit

Another electronic interface commonly used in piezoelectric energy harvesting is the SECE circuit [53, 54]. While the ability of power boosting of the SECE circuit is less significant than the SSHI circuits, it offers an advantage that harvested power is independent of the external load. This gives great vantage in the back-end interface design. Precisely, Fig. 6 shows the SECE circuit used in piezoelectric energy harvesting. It is followed by a full-bridge rectifier, consists of an inductor L_{SECE}, a switch

Copyright © 2014 by ASME

Downloaded From: http://proceedings.asmedigitalcollection.asme.org/ on 08/12/2017 Terms of Use: http://www.asme.org/about-asme/terms-of-use

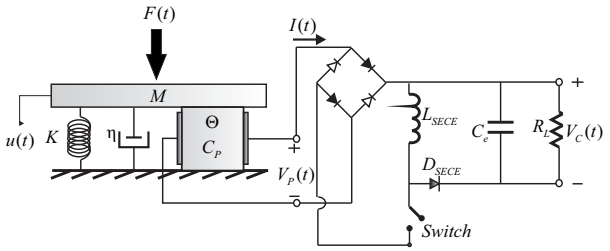

Figure 6. The parameter model of piezoelectric energy harvester connected to the SECE interface circuit.

S, and a rectifying diode D_{SECE}. The switch S is closed for a very short time when the oscillator's displacement reaches the extreme, giving energy transfer from the inductor L_{SECE} to the load R_L.

Using the balance of charge in the proposed voltage model as in Eq. (3), the output DC voltage V_c and the magnitude of equivalent voltage $\bar{V}_p^*$ is related to [55]

$$V_c^{\text{SECE}} = \left(2q_I^{\frac{1}{2}}\right)\bar{V}_p^*, \tag{19}$$

where q_I is the normalized electric quality factor similar to that defined in the SSHI circuits. But different from the previous interface circuits, the harvested average power is

$$P_{\text{harvested}} = \frac{\frac{1}{2}C_pV_c^2}{\frac{T}{2}} = \left(\frac{w}{2\pi}\right)C_pV_c^2, \tag{20}$$

where $T = \frac{2\pi}{w}$ is the period of oscillation.

It can be shown that the magnitude of displacement in the SECE case is [56]

$$|\bar{u}| = \frac{\bar{F}}{\left\{\left(K - w^2M + \frac{\Theta^2}{C_p}\right)^2 + \left(w\eta + \frac{4\Theta^2}{\pi C_p}\right)^2\right\}^{\frac{1}{2}}}. \tag{21}$$

The comparison of it with Eq. (14) gives the equivalent load impedance Z_2 of SECE interface by

$$Y_{2\text{R}}^{\text{SECE}} = \frac{4C_pw}{\pi}, \quad Y_{2\text{I}}^{\text{SECE}} = 0, \tag{22}$$

where $Y_{2\text{R}}$ and $-Y_{2\text{I}}$ are the real and imaginary parts of the complex impedance $\frac{1}{Z_2}$ as in Eq. (13). Different from the expression of equivalent load impedance in Eq. (16), Eq. (17) and Eq. (18) for the standard, parallel-SSHI and series-SSHI interfaces, the equivalent load impedance of the SECE circuit in Eq. (22) is independent from the load R_L, as expected. Finally, the FEM model of the SECE case is schematically identical to Fig. 4 and Fig. 5 for the cases of a single oscillator and an array of piezoelectric oscillators except that the equivalent load impedance is replaced by Eq. (22).

Conclusions

A direct finite element approach is proposed for designing piezoelectric energy harvesters accounting for the effect of nonlinear rectified interface circuits, such as the standard and parallel-/series-SSHI interfaces. It is shown that the attached energy harvesting circuit can be replaced by an equivalent load impedance in series with the negative piezoelectric capacitance. Fig. 4 and Fig. 5 schematically present the proposed finite element models for the cases of a single oscillator and multiple oscillators connected in series, respectively. As the explicit expression of equivalent load impedance is derived for each common interface circuit, the proposed framework provides a direct simulation without resorting to circuit solvers. Finally, the model is extended to the consideration of the SECE electronic interface whose merit is the independence of harvested power on external loads.

Acknowledgments

The authors are glad to acknowledge the partial supports from National Taiwan University and from Ministry of Science and Technology under Grant No 102-2221-E-002-126-MY3.

REFERENCES

[1] L. C. Rome, L. Flynn, E. M. Goldman, and T. D. Yoo. Generating Electricity while Walking with Loads. *Science*, **309**:1725–1728, 2005.

[2] A. D. Kuo. Harvesting Energy by Improving the Economy of Human Walking. *Science*, **309**:1686–1687, 2005.

[3] A. Erturk and D. J. Inman. *Piezoelectric Energy Harvesting*. Wiley, 2011.

[4] A. Erturk and D. J. Inman. Issues in Mathematical Modeling of Piezoelectric Energy Harvesters. *Smart Materials and Structures*, **17**:065016, 2008.

[5] H. A. Sodano, G. Park, and D. J. Inman. Estimation of Electric Charge Output for Piezoelectric Energy Harvesting. *Journal of Strain*, **40**:49–58, 2004.

[6] H. A. Sodano, D. J. Inman, and G. Park. A Review of Power Harvesting from Vibration Using Piezoelectric Materials. *The Shock and Vibration Digest*, **36**:197–205, 2004.

[7] N. E. duToit, B. L. Wardle, and S. G. Kim. Design Considerations for MEMS-Scale Piezoelectric Mechanical Vibration Energy Harvesters. *Integrated Ferroelectrics*, **71**:121–160, 2005.

[8] J. R. Liang and W. H. Liao. Energy Flow in Piezoelectric

 Copyright © 2014 by ASME

Downloaded From: http://proceedings.asmedigitalcollection.asme.org/ on 08/12/2017 Terms of Use: http://www.asme.org/about-asme/terms-of-use

Energy Harvesting Systems. *Smart Materials and Structures*, **20**:015005, 2011.
[9] S. Roundy and P. K. Wright. A Piezoelectric Vibration Based Generator for Wireless Electronics. *Smart Materials and Structures*, **13**:1131–1142, 2004.
[10] T. T. Yen, T. Hirasawa, P. K. Wright, A. P. Pisano, and L. Lin. Corrugated Aluminum Nitride Energy Harvesters for High Energy Conversion Effectiveness. *Journal of Micromechanics and Microengineering*, **21**:085037, 2011.
[11] S. Priya. Modeling of Electric Energy Harvesting Using Piezoelectric Windmill. *Applied Physics Letters*, **87**:184101, 2005.
[12] S. F. Ali, M. I. Friswell, and S. Adhikari. Piezoelectric Energy Harvesting with Parametric Uncertainty. *Smart Materials and Structures*, **19**:105010, 2010.
[13] T. Seuaciuc-Osorio and M. F. Daqaq. On the Reduced-Order Modeling of Energy Harvesters. *Journal of Intelligent Material Systems and Structures*, **20**:2003–2016, 2009.
[14] J. M. Dietl and E. Garcia. Beam Shape Optimization for Power Harvesting. *Journal of Intelligent Material Systems and Structures*, **21**:633–646, 2010.
[15] M. A. Karamia and D. J. Inman. Experimental and Analytical Parametric Study of Single-Crystal Unimorph Beams for Vibration Energy Harvesting. *IEEE Transaction on Ultrasonics, Ferroelectrics, and Frequency Control*, **58**:1508–1520, 2011.
[16] A. Mathers, K. S. Moon, and J. Yi. A Vibration-Based PMN-PT Energy Harvester. *IEEE Sensors Journal*, **9**:731–739, 2009.
[17] H. Takeda, K. Mihara, T. Yoshimura, T. Hoshina, and T. Tsurumi. Effect of Material Constants on Power Output in Piezoelectric Vibration-Based Generators. *IEEE Transaction on Ultrasonics, Ferroelectrics, and Frequency Control*, **58**:1852–1859, 2011.
[18] S. R. Oh, T. C. Wong, C. Y. Tan, K. Yao, and F. E. Tay. Fabrication of Piezoelectric Polymer Multilayers on Flexible Substrates for Energy Harvesting. *Smart Materials and Structures*, **23**:015013, 2014.
[19] H. J. Song, Y.T. Choi, N. M. Wereley, and A. S. Purekar. Energy Harvesting Devices Using Macro-fiber Composite Materials. *Journal of Intelligent Material Systems and Structures*, **21**:647–658, 2010.
[20] Y. C. Shu and I. C. Lien. Analysis of Power Output for Piezoelectric Energy Harvesting Systems. *Smart Materials and Structures*, **15**:1499–1512, 2006.
[21] Y. C. Shu and I. C. Lien. Efficiency of Energy Conversion for a Piezoelectric Power Harvesting System. *Journal of Micromechanics and Microengineering*, **16**:2429–2438, 2006.
[22] Y. C. Shu, I. C. Lien, and W. J. Wu. An Improved Analysis of the SSHI Interface in Piezoelectric Energy Harvesting. *Smart Materials and Structures*, **16**:2253–2264, 2007.
[23] I. C. Lien, Y. C. Shu, W. J. Wu, S. M. Shiu, and H. C. Lin. Revisit of Series-SSHI with Comparisons to Other Interfacing Circuits in Piezoelectric Energy Harvesting. *Smart Materials and Structures*, **19**:125009, 2010.
[24] G. K. Ottman, H. F. Hofmann, A. C. Bhatt, and G. A. Lesieutre. Adaptive Piezoelectric Energy Harvesting Circuit for Wireless Remote Power Supply. *IEEE Transactions on Power Electronics*, **17**:669–676, 2002.
[25] D. Guyomar, A. Badel, E. Lefeuvre, and C. Richard. Toward Energy Harvesting Using Active Materials and Conversion Improvement by Nonlinear Processing. *IEEE Transaction on Ultrasonics, Ferroelectrics, and Frequency Control*, **52**:584–595, 2005.
[26] A. Badel, A. Benayad, E. Lefeuvre, L. Lebrun, C. Richard, and D. Guyomar. Single Crystals and Nonlinear Process for Outstanding Vibration-Powered Electrical Generators. *IEEE Transaction on Ultrasonics, Ferroelectrics, and Frequency Control*, **53**:673–684, 2006.
[27] M. Lallart and D. Guyomar. An Optimized Self-Powered Switching Circuit for Non-Linear Energy Harvesting with Low Voltage Output. *Smart Materials and Structures*, **17**:035030, 2008.
[28] M. J. Guan and W. H. Liao. Characteristics of Energy Storage Devices in Piezoelectric Energy Harvesting Systems. *Journal of Intelligent Material Systems and Structures*, **19**:671–680, 2008.
[29] J. R. Liang and W. H. Liao. Impedance Modeling and Analysis for Piezoelectric Energy Harvesting Systems. *IEEE/ASME Transactions on Mechatronics*, **17**:1145–1157, 2012.
[30] W. J. Wu, A. M. Wickenheiser, T. Reissman, and E. Garcia. Modeling and Experimental Verification of Synchronized Discharging Techniques for Boosting Power Harvesting from Piezoelectric Transducers. *Smart Materials and Structures*, **18**:055012, 2009.
[31] A. M. Wickenheiser and E. Garcia. Power Optimization of Vibration Energy Harvesters Utilizing Passive and Active Circuits. *Journal of Intelligent Material Systems and Structures*, **21**:1343–1361, 2010.
[32] J. T. Scruggs. An Optimal Stochastic Control Theory for Distributed Energy Harvesting Networks. *Journal of Sound and Vibration*, **320**:707–725, 2009.
[33] H. P. Hu, Z. J. Cui, and J. G. Cao. Performance of a Piezoelectric Bimorph Harvester with Variable Width. *Journal of Mechanics*, **23**:197–202, 2007.
[34] S. Paquin and Y. St-Amant. Improving the Performance of a Piezoelectric Energy Harvester Using a Variable Thickness Beam. *Smart Materials and Structures*, **19**:105020, 2010.
[35] C. Mo, L. J. Radziemski, and W. W. Clark. Analysis of Piezoelectric Circular Diaphragm Energy Harvesters for Use in a Pressure Fluctuating System. *Smart Materials and Structures*, **19**:025016, 2010.
[36] C. J. Rupp, A. Evgrafov, K. Maute, and M. L. Dunn. Design of Piezoelectric Energy Harvesting Systems: A Topology Optimization Approach Based on Multilayer Plates and Shells. *Journal of Intelligent Material Systems and Structures*, **20**:1923–1939, 2009.
[37] M. A. Karamia and D. J. Inman. Electromechanical Modeling of the Low-Frequency Zigzag Micro-Energy Harvester. *Journal of Intelligent Material Systems and Structures*, **22**:271–282, 2011.
[38] E. S. Leland and P. K. Wright. Resonance Tuning of Piezoelectric Vibration Energy Scavenging Generators Using Compressive Axial Preload. *Smart Materials and Structures*, **15**:1413–1420, 2006.
[39] A. Erturk, J. M. Renno, and D. J. Inman. Modeling of Piezoelectric Energy Harvesting from an L-shaped Beam-mass Structure with an Application to UAVs. *Journal of Intelligent Material Systems and Structures*, **20**:529–544, 2009.
[40] D. J. Morris, J. M. Youngsman, M. J. Anderson, and D. F. Bahr. A Resonant Frequency Tunable, Extensional Mode Piezoelectric Vibration Harvesting Mechanism. *Smart Materials and Structures*, **17**:065021, 2008.

 Copyright © 2014 by ASME

Downloaded From: http://proceedings.asmedigitalcollection.asme.org/ on 08/12/2017 Terms of Use: http://www.asme.org/about-asme/terms-of-use

[41] I. C. Lien and Y. C. Shu. Array of Piezoelectric Energy Harvesting by Equivalent Impedance Approach. *Smart Materials and Structures*, **21**:082001, 2012.
[42] H. C. Lin, P. H. Wu, I. C. Lien, and Y. C. Shu. Analysis of an Array of Piezoelectric Energy Harvesters Connected in Series. *Smart Materials and Structures*, **22**:094026, 2013.
[43] M. Ferrari, V. Ferrari, M. Guizzetti, D. Marioli, and A. Taroni. Piezoelectric Multifrequency Energy Converter for Power Harvesting in Autonomous Microsystems. *Sensors and Actuators A*, **142**:329–335, 2008.
[44] H. J. Song, Y. T. Choi, A. S. Purekar, and N. M. Wereley. Performance Evaluation of Multi-tier Energy Harvesters Using Macro-fiber Composite Patches. *Journal of Intelligent Material Systems and Structures*, **20**:2077–2088, 2009.
[45] H. Xue, Y. T. Hu, and Q. M. Wang. Broadband Piezoelectric Energy Harvesting Devices Using Multiple Bimorphs with Different Operating Frequencies. *IEEE Transaction on Ultrasonics Ferroelectrics and Frequency Control*, **55**:2104–2108, 2008.
[46] Z. Yang and J. Yang. Connected Vibrating Piezoelectric Bimorph Beams as a Wide-band Piezoelectric Power Harvester. *Journal of Intelligent Material Systems and Structures*, **20**:569–574, 2009.
[47] S. M. Shahruz. Design of Mechanical Band-Pass Filters with Large Frequency Bands for Energy Scavenging. *Mechatronics*, **16**:523–531, 2006.
[48] M. Zhu, E. Worthington, and J. Njuguna. Analyses of Power Output of Piezoelectric Energy-Harvesting Devices Directly Connected to a Load Resistor Using a Coupled Piezoelectric-Circuit Finite Element Method. *IEEE Transaction on Ultrasonics Ferroelectrics and Frequency Control*, **56**:1309–1318, 2009.
[49] C. D. M. Junior, A. Erturk, and D. J. Inman. An Electromechanical Finite Element Model for Piezoelectric Energy Harvester Plates. *Journal of Sound and Vibration*, **327**:9–25, 2009.
[50] N. G. Elvin and A. A. Elvin. A Coupled Finite Element Circuit Simulation Model for Analyzing Piezoelectric Energy Generators. *Journal of Intelligent Material Systems and Structures*, **20**:587–595, 2009.
[51] Y. Yang and L. Tang. Equivalent Circuit Modeling of Piezoelectric Energy Harvesters. *Journal of Intelligent Material Systems and Structures*, **20**:2223–2235, 2009.
[52] P. H. Wu and Y. C. Shu. Finite Element Modeling of Piezoelectric Energy Harvesters. In W. H. Liao, editor, *Proceedings of SPIE: Active and Passive Smart Structures and Integrated Systems*, volume **9057**, page 90571D, 2014.
[53] E. Lefeuvre, A. Badel, C. Richard, and D. Guyomar. Piezoelectric Energy Harvesting Device Optimization by Synchronous Electric Charge Extraction. *Journal of Intelligent Material Systems and Structures*, **16**:865–876, 2005.
[54] E. Lefeuvre, A. Badel, C. Richard, L. Petit, and D. Guyomar. A Comparison between Several Vibration-Powered Piezoelectric Generators for Standalone Systems. *Sensors and Actuators A*, **126**:405–416, 2006.
[55] P. H. Wu. Analysis of Mixed Parallel and Series Connection of Piezoelectric Energy Harvesters with Experimental Validation. Ph.D. Thesis. *National Taiwan Univesity*, 2015.
[56] L. Tang and Y. Yang. Analysis of Synchronized Charge Extraction for Piezoelectric Energy Harvesting. *Smart Materials and Structures*, **20**:085022, 2011.

Copyright © 2014 by ASME

Downloaded From: http://proceedings.asmedigitalcollection.asme.org/ on 08/12/2017 Terms of Use: http://www.asme.org/about-asme/terms-of-use